Quantum Heisenberg-Ising models on generalized Fibonacci lattices

J. Q. You*
Chinese Center of Advanced Science and Technology (World Laboratory), P.O. Box 8730, Beijing 100080, China;
Laboratory of Atomic Imaging of Solids, Institute of Metal Research, Academia Sinica,
72 Wenhua Road, Shenyang 110015, China;
and Department of Physics, Xiangtan University, Xiangtan 411105, China

Xiaobiao Zeng† and Tiansheng Xie
Laboratory of Atomic Imaging of Solids, Institute of Metal Research, Academia Sinica, 72 Wenhua Road, Shenyang 110015, China

J. R. Yan
Chinese Center of Advanced Science and Technology (World Laboratory), P.O. Box 8730, Beijing 100080, China
and Department of Physics, Xiangtan University, Xiangtan 411105, China
(Received 28 August 1990; revised manuscript received 4 January 1991)

We study the quantum Heisenberg-Ising models on generalized Fibonacci lattices by the dynamical-maps technique, in which the nearest-neighbor Ising interactions take two values that follow successively the generalized Fibonacci sequences. The energy spectra are Cantor-like, and the wave functions are generally critical. It is further shown that the energy spectra do not have uniform scalings and that for some systems the wave functions are extended or localized in certain energy regions. In addition, we also obtain the critical lines of the quasiperiodic quantum Heisenberg-Ising models.

I. INTRODUCTION

There has been considerable interest in quasiperiodic systems, and much effort has been devoted to the study of quasiperiodic systems in one dimension. Particularly, a well-investigated one-dimensional (1D) quasiperiodic system is the Fibonacci structure, and most studies are concerned with the electronic, phonon, and magnetic properties.[1-7] For this quasiperiodic system, Kohmoto and coworkers[1] developed a dynamical-maps technique, which is successful in explaining the energy spectrum, wave functions, and some of the scaling properties of the system. Now this technique has been widely used to study the physical properties of the Fibonacci quasiperiodic systems.

Recently, generalized Fibonacci quasiperiodic systems have received much theoretical attention.[8-15] In their investigations of the electronic properties of the generalized Fibonacci quasiperiodic systems, Gumbs and Ali[8] derived several discrete dynamical maps for some generalized Fibonacci quasiperiodic systems. Motivated by their results, You and co-workers[14] obtained a unified trace map for all the generalized Fibonacci quasiperiodic systems, which is the generalization of the well-known Kohmoto-Kadanoff-Tang (KKT) trace map.[1] As Fibonacci structures, the generalized Fibonacci quasiperiodic systems are intermediate between periodic crystals and the random or disordered structures. However, the studies showed that these systems exhibit richer physical properties than the Fibonacci quasiperiodic system. The underlying lattices of the generalized Fibonacci quasiperiodic systems are the generalized Fibonacci lattices, which are, in some sense, a generalization of the Fibonacci lattice. The separation of successive lattice points of a generalized Fibonacci lattice takes value A or B and the sequence of tiles A and B is a generalized Fibonacci sequence that is constructed by the recursion relation $S_{l+1}=\{S_l^n|S_{l-1}^m\}$ with $S_0=\{B\}$ and $S_1=\{A\}$, in which $l\geq 1$, and m and n are positive integers. From the construction rule of S_l it follows that the total number F_l of tiles A and B in S_l satisfies the recursion relation $F_{l+1}=mF_{l-1}+nF_l$ for $l\geq 1$ with $F_0=F_1=1$. In the limit $l\rightarrow\infty$, the ratio of successive generalized Fibonacci numbers F_{l+1}/F_l tends to $\tau(m,n)=\frac{1}{2}[(n^2+4m)^{1/2}+n]$. The ratio F_{l+1}/F_l is an optimal rational approximant to $\tau(m,n)$.

In this paper, we study the quantum Heisenberg-Ising models on the generalized Fibonacci lattices in which the nearest-neighbor Ising interactions follow successively the generalized Fibonacci sequences. In Sec. II, we express the model Hamiltonian in the fermionic representation and present the dynamical maps. Section III concerns the Cantor-like energy spectra that are determined by the dynamical maps. The wave functions of the systems are studied in Sec. IV, and are divided into three kinds, i.e., the critical, extended, and localized wave functions. Section V describes the magnetic phase transition in the quasiperiodic quantum Heisenberg-Ising model. Finally, the results are summarized in Sec. VI.

II. THE MODEL

In this section, we focus our attention on the Hamiltonian of the quantum Heisenberg-Ising model and the

dynamical maps. In Sec. II A, following the ideas of Leib, Schultz, and Mattis,[16] we express the model Hamiltonian in the fermionic representation, and give the dynamical maps in Sec. II B.

A. Model Hamiltonian

We consider the following quantum Heisenberg-Ising model with only nearest-neighbor interactions:

$$H=\sum_{i=1}^{N}\mathbf{S}_{2i-1}\cdot\mathbf{S}_{2i}+2\sum_{i=1}^{N-1}\lambda_i S_{2i}^z S_{2i+1}^z \ . \tag{1}$$

Here the model is composed of $2N$ spins arranged in a row. The interactions are alternating Ising and isotropic Heisenberg interactions, and the coupling λ_i characterizes the relative strength of the two types of nearest-neighbor interactions. For the two kinds of tiles A and B in a two-tile sequence, each tile is decorated with two spins, of which one is put at the left end of the tile, and the other is located at the position which has a distance c away from the left end of the tile and d_i away from the right end. For all tiles c's are assigned to be constant and the associated couplings in the nearest-neighbor isotropic Heisenberg interactions are then equal to one another, as chosen here as one for simplicity. The quantity d_i is assigned to be d_A for tile A and d_B for tile B and then the coupling λ_i in the nearest-neighbor Ising interaction takes value λ_A or λ_B, associated with the two spacings d_A and d_B, respectively. If the two kinds of tiles A and B are distributed according to a generalized Fibonacci sequence S_∞ that is generated by the recursion relation $S_{l+1}=\{S_l^n|S_{l-1}^m\}$ with initial conditions $S_0=\{B\}$ and $S_1=\{A\}$, then there is $N\to\infty$ and the couplings λ_i are also arranged successively following the generalized Fibonacci sequence which is constructed by the same recursion relation with only different initial conditions $S_0=\{\lambda_B\}$ and $S_1=\{\lambda_A\}$. For instance, for the Fibonacci sequence with $(m,n)=(1,1)$, the couplings $\{\lambda_i\}$ are arranged this way:

$$\lambda_A\lambda_B\lambda_A\lambda_A\lambda_B\lambda_A\lambda_B\lambda_A\lambda_A\lambda_B\lambda_A\lambda_A\lambda_B\cdots \ ,$$

while both the couplings in the nearest-neighbor isotropic Heisenberg interactions and those in the nearest-neighbor Ising interactions are arranged in the following way:

$$1\lambda_A 1\lambda_B 1\lambda_A 1\lambda_A 1\lambda_B 1\lambda_A 1\lambda_B 1\lambda_A 1\lambda_A 1\lambda_B 1\lambda_A 1\lambda_A 1\lambda_B\cdots$$

For the ith pair of spins, we introduce the four eigenfunctions of $\mathbf{S}_{2i-1}\cdot\mathbf{S}_{2i}$:

$$\Phi_{1,1}^i=\uparrow\uparrow, \quad \Phi_{1,-1}^i=\downarrow\downarrow \ , \tag{2a}$$

and

$$\Phi_{1,0}^i=\frac{1}{\sqrt{2}}(\downarrow\uparrow+\uparrow\downarrow), \quad \Phi_{0,0}^i=\frac{1}{\sqrt{2}}(\downarrow\uparrow-\uparrow\downarrow) \ , \tag{2b}$$

where the first and second arrows refer to the $(2i-1)$th and $2i$th spins, respectively, and the first and second subscripts of Φ^i refer to the quantum numbers J_i and M_i, respectively. Since the application of either $S_{2i-2}^z S_{2i-1}^z$ or $S_{2i}^z S_{2i+1}^z$ to any of the above four states leaves M_i unchanged, a 2^{2N}-dimensional subspace for all states is then defined as one of the three possible values $0,\pm1$ assigned to each of the N M_i's. In this paper we consider the ground state that is in the subspace with $M_i=0$ for all i.

Introducing the raising and lowering operators $a_i^\dagger$ and a_i for the ith pair of spins,

$$a_i^\dagger\Phi_{0,0}^i=\Phi_{1,0}^i, \quad a_i^\dagger\Phi_{1,0}^i=0 \ , \tag{3a}$$

and

$$a_i\Phi_{0,0}^i=0 \ , \quad a_i\Phi_{1,0}^i=\Phi_{0,0}^i \ , \tag{3b}$$

the Hamiltonian (1) can be cast in the form[16]

$$H=-3N/4+\sum_{i=1}^{N}a_i^\dagger a_i - \tfrac{1}{2}\sum_{i=1}^{N-1}\lambda_i[(a_i^\dagger a_{i+1}+a_i^\dagger a_{i+1}^\dagger)+\text{H.c.}] \ . \tag{4}$$

The operators $a_i^\dagger$ and a_i partly resemble fermionic and bosonic operators, respectively, since there are relations

$$\{a_i,a_i^\dagger\}\equiv a_i a_i^\dagger+a_i^\dagger a_i=1, \quad a_i^2=(a_i^\dagger)^2=0 \ , \tag{5a}$$

and

$$[a_i^\dagger,a_j]\equiv a_i^\dagger a_j-a_j a_i^\dagger=0, \quad [a_i^\dagger,a_j^\dagger]=[a_i,a_j]=0 \ , \tag{5b}$$

Let

$$c_i\equiv\exp\left[\pi i\sum_{j=1}^{i-1}a_j^\dagger a_j\right]a_i \tag{6a}$$

and

$$c_i^\dagger\equiv a_i^\dagger\exp\left[-\pi i\sum_{j=1}^{i-1}a_j^\dagger a_j\right] \ , \tag{6b}$$

where c_i and $c_i^\dagger$ are anticommuting fermionic operators:

$$\{c_i,c_j^\dagger\}=\delta_{ij}, \quad \{c_i,c_j\}=\{c_i^\dagger,c_j^\dagger\}=0 \ . \tag{7}$$

In the fermionic representation, Eq. (4) is further written as

$$H=\sum_{i=1}^{N}c_i^\dagger c_i-\tfrac{1}{2}\sum_{i=1}^{N-1}\lambda_i[(c_i^\dagger c_{i+1}+c_i^\dagger c_{i+1}^\dagger)+\text{H.c.}] \ , \tag{8}$$

where the quantity $-3N/4$ is chosen to be the zero point of the total energy of the system.

The c-cyclic treatment[16] is carried out by letting $\sum_i^{N-1}\to\sum_i^N$ in the second summation of Eq. (8) and having $c_{N+1}\equiv c_1$ and $c_{N+1}^\dagger\equiv c_1^\dagger$ (the periodic boundary condition). The Hamiltonian can then be expressed, in the quadratic form, as

$$H=\sum_{i,j}[c_i^\dagger A_{ij}c_j+\tfrac{1}{2}(c_i^\dagger B_{ij}c_j^\dagger+\text{H.c.})] \ , \tag{9}$$

where $A=(A_{ij})$ and $B=(B_{ij})$ are symmetric and antisymmetric matrices, respectively, whose nonzero elements are $A_{ii}=1$, $A_{i,i+1}=-\lambda_i/2$, and $A_{1,N}=-\lambda_N/2$; $B_{i,i+1}=-\lambda_i/2$ and $B_{1,N}=\lambda_N/2$.

B. Dynamical maps

Eigenvalues of the Hamiltonian (9) are determined by the equations

$$(A+B)\phi=\Lambda\psi\ , \tag{10a}$$

$$(A-B)\psi=\Lambda\phi\ , \tag{10b}$$

which yield

$$\Lambda\psi_i=\phi_i-\lambda_i\phi_{i+1}\ , \tag{11a}$$

$$\Lambda\phi_i=-\lambda_{i-1}\psi_{i-1}+\psi_i\ , \tag{11b}$$

where $\psi=(\psi_1\psi_2\cdots\psi_N)^t$ and $\phi=(\phi_1\phi_2\cdots\phi_N)^t$.

From Eqs. (11a) and (11b) we obtain the transfer-matrix equation

$$\Phi_{i+1}=M(i)\Phi_i\ , \tag{12}$$

where the wave function Φ_i is a column vector $(\phi_i,\psi_i)^t$ and the transfer matrix is a 2×2 unimodular matrix

$$\underline{M}(i)=\begin{bmatrix}1/\lambda_i & -\Lambda/\lambda_i\\ \Lambda/\lambda_i & (\lambda_i^2-\Lambda^2)/\lambda_i\end{bmatrix}\ , \tag{13}$$

which is

$$\underline{M}(A)=\begin{bmatrix}1/\lambda_A & -\Lambda/\lambda_A\\ \Lambda/\lambda_A & (\lambda_A^2-\Lambda^2)/\lambda_A\end{bmatrix} \tag{14a}$$

or

$$\underline{M}(B)=\begin{bmatrix}1/\lambda_B & -\Lambda/\lambda_B\\ \Lambda/\lambda_B & (\lambda_B^2-\Lambda^2)/\lambda_B\end{bmatrix} \tag{14b}$$

as the coupling λ_i takes value λ_A or λ_B. The wave function for the arbitrary (N_s+1)th pair of spins is given by

$$\Phi_{N_s+1}=\underline{M}^{(N_S)}\Phi_1\ , \tag{15}$$

where

$$\underline{M}^{(N_s)}=\underline{M}(N_s)\underline{M}(N_s-1)\cdots\underline{M}(2)\underline{M}(1) \tag{16}$$

is successive multiplications of the transfer matrices.

If $\{\lambda_i\}$ is a generalized Fibonacci sequence, $\{\underline{M}(i)\}$ are also arranged like the generalized Fibonacci sequence. It can be shown that the transfer matrix $\underline{M}_l\equiv\underline{M}^{(F_l)}$, in which F_l is a generalized Fibonacci number, obeys the recursion relation

$$\underline{M}_{l+1}=\underline{M}_{l-1}^{m}\underline{M}_l^{n} \tag{17}$$

with initial conditions $\underline{M}_0=\underline{M}(B)$ and $\underline{M}_1=\underline{M}(A)$.

From theory of matrices the Nth power of a 2×2 unimodular matrix $\underline{M}_l$ is given by[17]

$$\underline{M}_l^N=\begin{bmatrix}a_l\mathcal{U}_{N-1}(x_l)-\mathcal{U}_{N-2}(x_l) & b_l\mathcal{U}_{N-1}(x_l)\\ c_l\mathcal{U}_{N-1}(x_l) & d_l\mathcal{U}_{N-1}(x_l)-\mathcal{U}_{N-2}(x_l)\end{bmatrix}\ , \tag{18}$$

where

$$\underline{M}_l=\begin{bmatrix}a_l & b_l\\ c_l & d_l\end{bmatrix}\ ,\quad x_l\equiv\tfrac{1}{2}\mathrm{Tr}\underline{M}_l=\tfrac{1}{2}(a_l+d_l)\ , \tag{19}$$

in which Tr denotes the trace of a matrix, and $\mathcal{U}(x_l)$ is the Nth Chebyshev polynomial of the second kind:

$$\mathcal{U}(x_l)=\frac{\sin[(N+1)\cos^{-1}(x_l)]}{\sin[\cos^{-1}(x_l)]}\ , \tag{20}$$

which satisfies the recursion relation

$$\mathcal{U}_N(x_l)=2x_l\mathcal{U}_{N-1}(x_l)-\mathcal{U}_{N-2}(x_l)\ . \tag{21}$$

From Eq. (17) one has

$$(\underline{M}_{l-2}^{-1})^m=\underline{M}_{l-1}^{n}\underline{M}_l^{-1}\ . \tag{22}$$

Using relation (18) and taking the trace of Eqs. (17) and (22), respectively, we obtain the trace map for the generalized Fibonacci lattices,[14]

$$\begin{aligned}x_{l+1}=\mathcal{U}_{n-1}(x_l)\mathcal{U}_{m-1}(x_{l-1})\Bigg[2x_lx_{l-1}-\left[\frac{\mathcal{U}_{m-2}(x_{l-1})}{\mathcal{U}_{m-1}(x_{l-1})}+\frac{\mathcal{U}_{n-2}(x_{l-1})}{\mathcal{U}_{n-1}(x_{l-1})}\right]x_l-\frac{\mathcal{U}_{n-2}(x_l)}{\mathcal{U}_{n-1}(x_l)}x_{l-1}\\ -\frac{\mathcal{U}_{m-1}(x_{l-2})}{\mathcal{U}_{n-1}(x_{l-1})}x_{l-2}+\left[\frac{\mathcal{U}_{m-2}(x_{l-2})}{\mathcal{U}_{n-1}(x_{l-1})}+\frac{\mathcal{U}_{n-2}(x_l)\mathcal{U}_{m-2}(x_{l-1})}{\mathcal{U}_{n-1}(x_l)\mathcal{U}_{m-1}(x_{l-1})}\right]\Bigg]\end{aligned} \tag{23}$$

with the following initial conditions:

$$x_0=\tfrac{1}{2}(\lambda_B+1/\lambda_B-\Lambda^2/\lambda_B)\ ,$$
$$x_1=\tfrac{1}{2}(\lambda_A+1/\lambda_A-\Lambda^2/\lambda_A)\ , \tag{24a}$$

and

$$x_2=\mathcal{U}_{n-1}(x_1)\mathcal{U}_{m-1}(x_0)[2x_1x_0-\tfrac{1}{2}(\lambda_A/\lambda_B+\lambda_B/\lambda_A)]$$
$$-\mathcal{U}_{n-1}(x_1)\mathcal{U}_{m-2}(x_0)x_1-\mathcal{U}_{n-2}(x_1)\mathcal{U}_{m-1}(x_0)x_0$$
$$+\mathcal{U}_{n-2}(x_1)\mathcal{U}_{m-2}(x_0)\ . \tag{24b}$$

Since $\underline{M}_l$ is a real 2×2 unimodular matrix, i.e., $\det\underline{M}_l=1$, in which det denotes the determinant of a matrix, it can be specified only by three real numbers. Thus the matrix map (17) can be considered to be a 6D discrete dynamical system. The trace map (23) is obtained by introducing the trace of $\underline{M}_l$, which is a reduced 3D dynamical system and can be regarded as the projection of the full 6D dynamical map (17) onto a 3D orbit. The energy spectrum of the quantum Heisenberg-Ising model on a generalized Fibonacci lattice is determined by the behavior of the trace map (23). Merely by studying it, one can obtain the energy spectrum of the quasiperiodic quantum Heisenberg-Ising model. Once the energy spectrum is determined, one can then obtain the wave function for a given energy lying in the spectrum by successive multiplications of the transfer matrices.

III. CANTOR-LIKE ENERGY SPECTRA

The quantum Heisenberg-Ising model on a generalized Fibonacci lattice can be approximated by the Heisenberg-Ising models on a sequence of periodic lattices with progressively larger unit cells of size F_l defined by the optimal rational approximants to $\tau(m,n)$. According to Bloch theorem, one has

$$\Phi_{F_l+1}=e^{iKF_l}\Phi_1\ , \tag{25}$$

where K is the wave vector and F_l the size of the unit cell of a periodic lattice. From Eq. (15) one also has

$$\Phi_{F_l+1}=\underline{M}_l\Phi_1=\begin{bmatrix}m_{11} & m_{12}\\ m_{21} & m_{22}\end{bmatrix}\Phi_1\ . \tag{26}$$

Thus it follows from Eqs. (25) and (26) that

$$\det\begin{bmatrix}m_{11}-e^{iKF_l} & m_{12}\\ m_{21} & m_{22}-e^{iKF_l}\end{bmatrix}=0\ , \tag{27}$$

which yields

$$\cos(KF_l)=\tfrac{1}{2}(m_{11}+m_{22})=x_l\ . \tag{28}$$

From Eq. (28) we then obtain the following conditions for bands and gaps, respectively, in the energy spectrum:

$$|x_l|\le1\ , \tag{29}$$
$$|x_l|>1\ . \tag{30}$$

Since the quantum Heisenberg-Ising models on the generalized Fibonacci lattices are obtained by the limit of $l\to\infty$, the energy spectra of these quasiperiodic models are thus given in the limit $l\to\infty$.

As typical examples, we present in Figs. 1(a)–1(d) the band structures of the quantum Heisenberg-Ising models on periodic lattices of periods $F_l=mF_{l-2}+nF_{l-1}$ for $l\ge2$ with $F_0=F_1=1$, in which $(m,n)=(1,1)$, (1,2), (2,1), and (3,1), respectively. The two types of couplings are chosen to be $K_A=1$ and $K_B=2$. One sees that each energy spectrum consists of F_l bands and F_l-1 gaps at the lth iteration. As l gets large, more gaps appear. In the limit $l\to\infty$, it can be concluded that the gaps are densely populated in the energy spectra of the quasiperiodic quantum Heisenberg-Ising models. Another feature is that the energy spectra is self-similar. The self-similarities and the dense distributions of gaps imply that the energy spectra of the quantum Heisenberg-Ising models on the generalized Fibonacci lattices are Cantor-like. In addition, it can also be seen that the energy spectra do not have uniform scalings. In Figs. 1(a) and 1(b), there are large bands and small gaps at low values of Λ, while for high values of Λ the bands are very narrow. At high

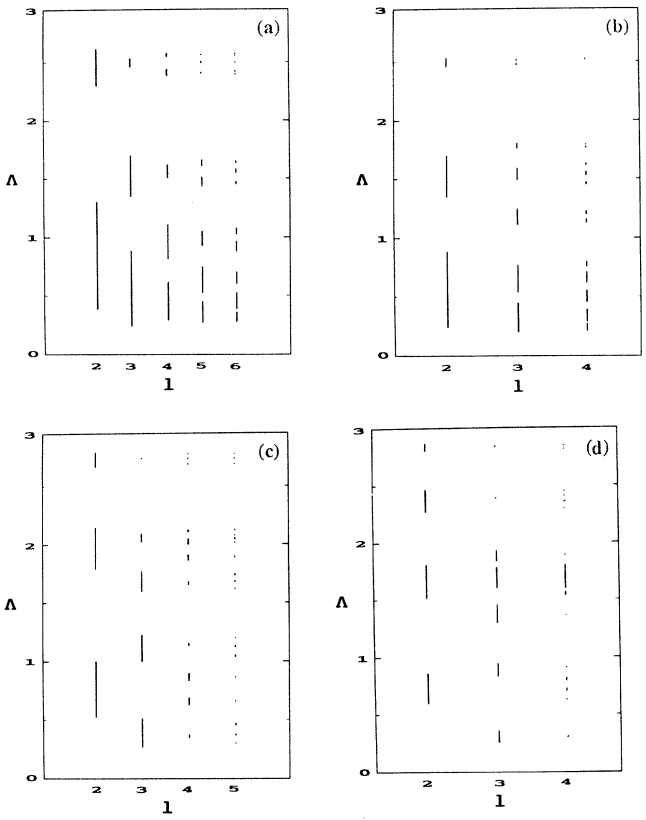

FIG. 1. Band structures of the quantum Heisenberg-Ising models on periodic lattices of periods $F_l=mF_{l-2}+nF_{l-1}$ for $l\ge2$ with $F_0=F_1=1$. (a) $m=1$, $n=1$, $l=2$, 3, 4, 5, and 6; (b) $m=1$, $n=2$, $l=2$, 3, and 4; (c) $m=2$, $n=1$, $l=2$, 3, 4, and 5; (d) $m=3$, $n=1$, $l=2$, 3, and 4. The two kinds of couplings are chosen to be $\lambda_A=1$ and $\lambda_B=2$. The band structures for larger l can be similarly obtained and the energy spectra of the quasiperiodic quantum Heisenberg-Ising models are given in the limit $l\to\infty$. Note that the coupling parameter λ has the same units as the energy Λ.

iterations of l, it is found in our numerical calculations that the gaps tend to vanish when Λ goes to the bottom edges $\Lambda_{\min}$ of the energy spectra. This indicates that the wave functions tend to be extended in the region $\Lambda \simeq \Lambda_{\min}$. As to Fig. 1(d) there are large bands and small gaps in the central part of the spectrum, and it is also found that as l gets large, the gaps tend to vanish in this region.

IV. CRITICAL, EXTENDED, AND LOCALIZED WAVE FUNCTIONS

For a given energy lying in the energy spectrum of the quantum Heisenberg-Ising model on a generalized Fibonacci lattice, one can numerically obtain the wave function from Eqs. (15) and (16), namely, by successive multiplications of the transfer matrices. Figures 2–5 are the numerically calculated wave functions of four systems composed of 1597, 1393, 1365, and 1159 pairs of spins, respectively. The two kinds of couplings are chosen to be $\lambda_A = 1$ and $\lambda_B = 2$.

Figure 2 is the wave functions of the system with $(m,n)=(1,1)$, which are numerically calculated at $\Lambda = 0.274\,855\,4$ and $1.556\,739$, respectively. The first energy is very close to the bottom edge $\Lambda_{\min}$ of the energy spectrum and the corresponding wave function is extended. The wave function calculated at $\Lambda = 1.556\,739$ is critical, i.e., self-similar and neither extended nor localized in a standard fashion. The wave functions of the system with $(m,n)=(1,2)$ are shown in Fig. 3, which are numerically calculated at $\Lambda = 0.205\,424$ and $1.627\,864$, respectively. Similar to those in Fig. 2, the wave function is extended at the first energy that is also very close to the bottom edge $\Lambda_{\min}$ of the energy spectrum, while that at the second energy is critical. The wave functions of the system with $(m,n)=(2,1)$ presented in Fig. 4 are calculated at $\Lambda = 1.140\,203$ and $2.021\,545\,172$, which are critical and localized, respectively. Figure 5 is the wave functions of the system with $(m,n)=(3,1)$ that are calculated at the energies $\Lambda = 0.911\,16$, 1.7, and $0.906\,637\,669$, respectively. The wave functions at $\Lambda = 0.911\,16$ and 1.7 are critical and extended, respectively, while that at $\Lambda = 0.906\,637\,669$ has three main peaks, of which each is localized as that shown in Fig. 4(b).

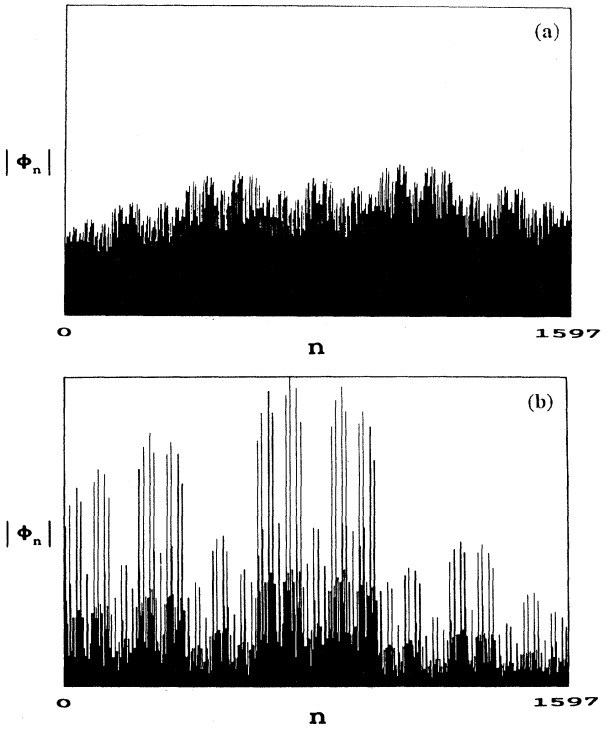

FIG. 2. Wave functions of the system with $(m,n)=(1,1)$. (a) Extended state, $\Lambda = 0.274\,855\,4$; (b) critical state, $\Lambda = 1.556\,739$. The system consists of 1597 pairs of spins and the two kinds of couplings are chosen to be $\lambda_A = 1$ and $\lambda_B = 2$.

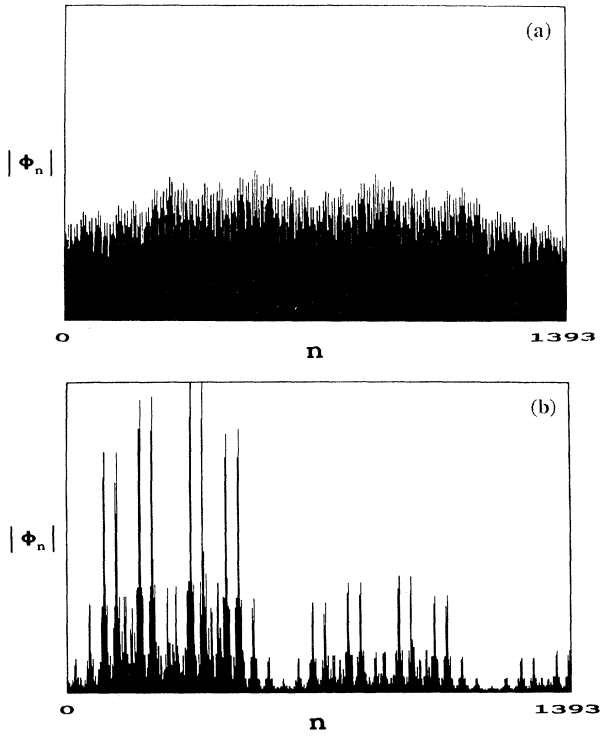

FIG. 3. Wave functions of the system with $(m,n)=(1,2)$. (a) Extended state, $\Lambda = 0.205\,424$; (b) critical state, $\Lambda = 1.627\,864$. The system consists of 1393 pairs of spins and the two kinds of couplings are chosen to be $\lambda_A = 1$ and $\lambda_B = 2$.

From the above numerical calculations, one sees that the wave functions shown in Figs. 2(a) and 3(a) are extended at the energies very close to the bottom edges of the energy spectra. We have also calculated the wave functions at other energies that are in the regions with $\Lambda \sim \Lambda_{\min}$ and found that the wave functions tend to be extended. The corresponding energy of the extended wave function shown in Fig. 5(b) is located in the middle part of the spectrum [see Fig. 1(d)]. In our calculations, we have also found that the wave functions are extended or tend to be extended at many energies in this central region. These conclusions agree with the speculations

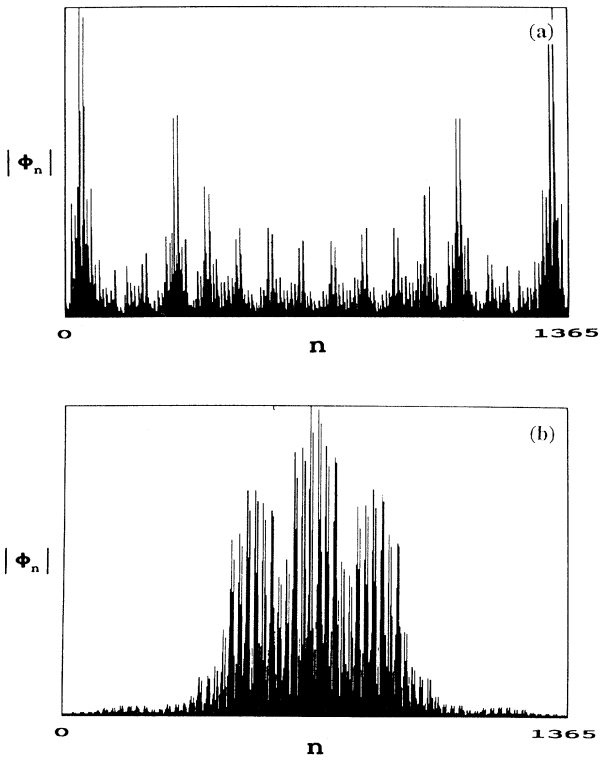

FIG. 4. Wave functions of the system with $(m,n)=(2,1)$. (a) Critical state, $\Lambda=1.140\,203$; (b) localized state, $\Lambda=2.021\,545\,172$. The system consists of 1365 pairs of spins and the two kinds of couplings are chosen to be $\lambda_A=1$ and $\lambda_B=2$.

based upon the characteristics of the energy spectra. The localized wave functions are found only in some extremely narrow regions for the systems with $(m,n)=(2,1)$ and (3,1). As to the critical wave functions, they are found in many regions. This implies that the criticality is still the main feature of the wave functions of the quantum Heisenberg-Ising models on the generalized Fibonacci lattices.

V. PHASE TRANSITION IN THE HEISENBERG-ISING MODEL

Similar to the periodic quantum Ising model, it is found[7,13,15] that the quasiperiodic quantum Ising model exhibits a magnetic phase transition driven by the zero mode of the Hamiltonian at a critical value of the coupling. Analogously, the quantum Heisenberg-Ising model on a generalized Fibonacci lattice may also undergo a phase transition for a critical value of the coupling, as what occurs in the periodic quantum Heisenberg-Ising model.[16] In the following, we denote the two types of couplings λ_A and λ_B, for convenience, as λ and $r\lambda$, respectively, and denote the critical value of the coupling as λ_c. As in the quasiperiodic quantum Ising model, the quantum-mechanical phase transition exhibited in the quasiperiodic quantum Heisenberg-Ising model should be driven by the zero mode of the Hamiltonian (9), which is given by

$$(A_c+B_c)\phi_0=0\ , \tag{31a}$$

$$(A_c-B_c)\psi_0=0\ , \tag{31b}$$

where A_c and B_c are the matrices A and B calculated at the critical value λ_c of the coupling. From Eqs. (11a) and (11b) it follows that

$$\phi_{0,i}-\lambda_{i,c}\phi_{0,i+1}=0\ , \tag{32a}$$

$$\psi_{0,i}-\lambda_{i-1,c}\psi_{0,i-1}=0,\ i=1,2,\ldots,F_l\ . \tag{32b}$$

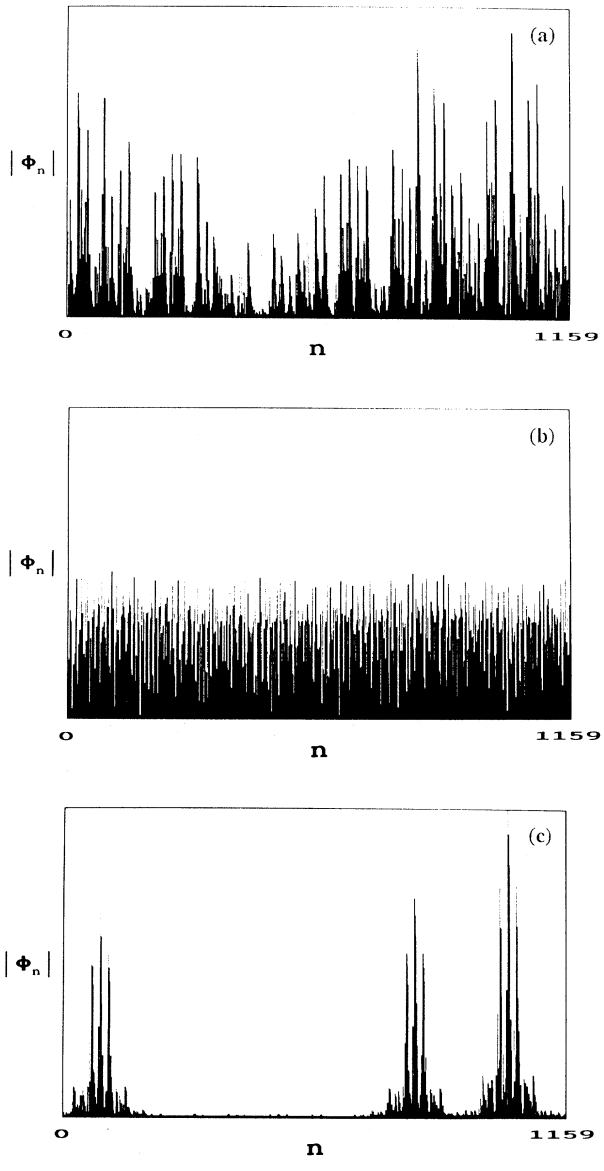

FIG. 5. Wave functions of the system with $(m,n)=(3,1)$. (a) Critical state, $\Lambda=0.911\,16$; (b) extended state, $\Lambda=1.7$; (c) localized state, $\Lambda=0.906\,637\,669$. The system consists of 1159 pairs of spins and the two kinds of couplings are chosen to be $\lambda_A=1$ and $\lambda_B=2$.

The solutions to these equations are

$$\phi_{0,j}=\phi_{0,F_l}\prod_{i=j}^{F_l-1}\lambda_{i,c}\ , \tag{33a}$$

$$\psi_{0,j}=\psi_{0,1}\prod_{i=1}^{j-1}\lambda_{i,c}\ , \tag{33b}$$

where $\lambda_{i,c}$ is either λ_c or $r\lambda_c$ depending on the position i in the quasiperiodic sequence.

From the periodic boundary condition $\Phi_{0,F_l+1}=\Phi_{0,1}$ we obtain

$$\lambda_c=|r|^{-1/(1+\sigma_l)}\ , \tag{34}$$

where $\sigma_l(m,n)=F_l^A/F_l^B$ in which F_l^A and F_l^B are, respectively, the total numbers of tiles A and B in the lth generation S_l of a generalized Fibonacci sequence. From the construction rule of the generalized Fibonacci sequences $S_{l+1}=\{S_l^n|S_{l-1}^m\}$ with $S_0=\{B\}$ and $S_1=\{A\}$, one can find that F_l^A and F_l^B obey the same recursion relation as F_l but with different initial conditions: $F_{l+1}^A=mF_{l-1}^A+nF_l^A$ with $F_0^A=0$ and $F_l^A=1$, and $F_{l+1}^B=mF_{l-1}^B+nF_l^B$ with $F_0^B=1$ and $F_1^B=0$. Since $F_{l+1}^B=mF_l^A$, we then obtain that $\sigma(m,n)=\lim_{l\to\infty}\sigma_l(m,n)=\tau(m,n)/m$. As $l\to\infty$, Eq. (34) becomes

$$\lambda_c=|r|^{-m/(m+\tau)}\ . \tag{35}$$

This is the critical line for the quantum Heisenberg-Ising model on a generalized Fibonacci lattice. Although the quantum Heisenberg-Ising model is different from the quantum Ising model, their critical lines are the same for the generalized Fibonacci lattices (see Refs. 13 and 15). Figure 6 presents the plots of the bottom edges $\Lambda_{\min}$ of the energy spectra of the systems with $(m,n)=(1,1)$, (1,2), (2,1), and (3,1). The pairs of spins are chosen to be 1597, 1393, 1365, and 1159, corresponding to $l=16$, 9, 11, and 9, respectively. At the critical values of the couplings given by Eq. (34), in which $r=2$, the bottom edges of the energy spectra fall down to $\Lambda_{\min}=0$. This result matches the speculation that the magnetic phase transition is driven by the zero mode of the Hamiltonian (9) at a critical value λ_c of the coupling.

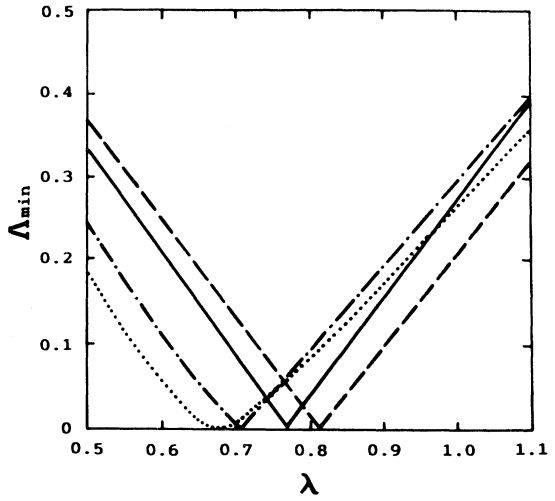

FIG. 6. Bottom edges $\Lambda_{\min}$ of the energy spectra of the systems with $(m,n)=(1,1)$, (1,2), (2,1), and (3,1), which are represented by solid, dashed, dot-dashed, and dotted lines, respectively. The pairs of spins are 1597, 1393, 1365, and 1159. The two kinds of couplings λ_A and λ_B are denoted by λ and $r\lambda$, in which r is chosen to be $r=2$. At the critical values λ_c of the couplings, the bottom edges fall down to $\Lambda_{\min}=0$.

VI. SUMMARY

The quantum Heisenberg-Ising models on the generalized Fibonacci lattices are studied by the dynamical-maps technique, in which the nearest-neighbor Ising interactions take two values that follow successively the generalized Fibonacci sequences. The energy spectra of the quasiperiodic quantum Heisenberg-Ising models are Cantor-like, i.e., they are self-similar and exhibit dense distributions of gaps, In addition, the energy spectra do not have uniform scalings. For some systems, there are some energy regions in which the bands are larger with vanishing gaps, yielding the spectra therein to be almost continuous.

The main feature of the wave functions is the criticality, since the critical wave functions, which are self-similar and neither extended nor localized, are found in many regions of the energy spectra. In the above-mentioned energy regions in which the spectra are almost continuous, it is found that the wave functions are extended or tend to be extended. For some systems, localized wave functions are also found. However, the corresponding energy regions are extremely narrow.

The quantum Heisenberg-Ising model on a generalized Fibonacci lattice undergoes a magnetic phase transition driven by the zero mode of the Hamiltonian at the critical value of the coupling. The critical lines are obtained for all generalized Fibonacci lattices, and it is numerically shown that the bottom edges of the energy spectra really fall down to zero at the critical values of the couplings.

ACKNOWLEDGMENTS

This work has been supported by the National Natural Science Foundation of China. One of the authors (J.Q.Y.) has also been supported by two grants, from the Laboratory of Atomic Imaging of Solids and the Beijing Laboratory of Electron Microscopy, Chinese Academy of Sciences.

*Present address: Laboratory of Modern Physics, Institute of Science and Technology, Xiangtan University, Xiangtan 411105, Hunan, China.

†Present address: Department of Materials Science and Engineering, Cornell University, Ithaca, New York 14853.

[1] M. Kohmoto, L. P. Kadanoff, and C. Tang, Phys. Rev. Lett. **50**, 1870 (1983); M. Kohmoto and J. R. Banavar, Phys. Rev. B **34**, 563 (1986); M. Kohmoto, B. Sutherland, and C. Tang,

ibid. **35**, 1020 (1987).
[2]S. Ostlund, R. Pandit, D. Rand, H. J. Schellnhuber, and E. Siggia, Phys. Rev. Lett. **50**, 1873 (1983).
[3]J. P. Lu, T. Odagaki, and J. L. Birman, Phys. Rev. B **33**, 4809 (1986); H. De Raedt and T. Schneider, Z. Phys. B **71**, 287 (1988).
[4]J. M. Luck and D. Petritis, J. Stat. Phys. **42**, 289 (1986).
[5]F. Nori and J. P. Rodriquez, Phys. Rev. B **34**, 2207 (1986); Q. Niu, and F. Nori, Phys. Rev. Lett. **57**, 2057 (1986).
[6]J. M. Luck and Th. M. Nieuwenhuizen, Europhys. Lett. **2**, 257 (1986); S. Xiong, J. Phys. C **20**, L167 (1987).
[7]M. M. Doria and I. I. Satija, Phys. Rev. Lett. **60**, 444 (1988); H. A. Ceccatto, *ibid.* **62**, 203 (1989); V. G. Benza, Europhys. Lett. **8**, 321 (1989).
[8]G. Gumbs and M. K. Ali, Phys. Rev. Lett. **60**, 1081 (1988); J. Phys. A **21**, L517 (1988); **22**, 951 (1989).
[9]M. Holzer, Phys. Rev. B **38**, 1709 (1988); **38**, 5756 (1988).
[10]M. Kolář and M. K. Ali, Phys. Rev. B **39**, 426 (1989); J. Phys. Condens. Matter **1**, 823 (1989).
[11]F. Wijnands, J. Phys. A **22**, 3267 (1989).
[12]M. Severin and R. Riklund, Phys. Rev. B **39**, 10 362 (1989); M. Severin, M. Dulea, and R. Riklund, J. Phys. Condens. Matter **1**, 8851 (1989).
[13]M. Kolář, M. K. Ali, and I. I. Satija, Phys. Rev. B **40**, 11 083 (1989).
[14]J. Q. You and Q. B. Yang, J. Phys. Condens. Matter **2**, 2093 (1990); J. Q. You, Q. B. Yang, and J. R. Yan, Phys. Rev. B **41**, 7491 (1990); J. Q. You, J. R. Yan, and Q. B. Yang, Z. Phys. B **80**, 119 (1990).
[15]J. Q. You and Q. B. Yang, Phys. Rev. B **41**, 7073 (1990).
[16]E. Leib, T. Schultz, and D. Mattis, Ann. Phys. (N.Y.) **16**, 407 (1961).
[17]M. Born and E. Wolf, *Principles of Optics*, 6th ed. (Pergamon, Oxford, 1980), p. 67.